Development 134, 567-578 (2007) doi:10.1242/dev.02748

Abelson kinase (Abl) and RhoGEF2 regulate actin organization during cell constriction in *Drosophila*

Donald T. Fox[1] and Mark Peifer[1,2,*]

Morphogenesis involves the interplay of different cytoskeletal regulators. Investigating how they interact during a given morphogenetic event will help us understand animal development. Studies of ventral furrow formation, a morphogenetic event during *Drosophila* gastrulation, have identified a signaling pathway involving the G-protein Concertina (Cta) and the Rho activator RhoGEF2. Although these regulators act to promote stable myosin accumulation and apical cell constriction, loss-of-function phenotypes for each of these pathway members is not equivalent, suggesting the existence of additional ventral furrow regulators. Here, we report the identification of Abelson kinase (Abl) as a novel ventral furrow regulator. We find that Abl acts apically to suppress the accumulation of both Enabled (Ena) and actin in mesodermal cells during ventral furrow formation. Further, RhoGEF2 also regulates ordered actin localization during ventral furrow formation, whereas its activator, Cta, does not. Taken together, our data suggest that there are two crucial preconditions for apical constriction in the ventral furrow: myosin stabilization/activation, regulated by Cta and RhoGEF2; and the organization of apical actin, regulated by Abl and RhoGEF2. These observations identify an important morphogenetic role for Abl and suggest a conserved mechanism for this kinase during apical cell constriction.

KEY WORDS: Fog, G-alpha 12, G-alpha 13, Abl, Cta, Neural tube, S2 cell, Adherens junction, *Drosophila*

INTRODUCTION

During embryogenesis, many morphogenetic events shape the body plan. These rely on shape changes in single cells that must be coordinated within tissues. Although the particular cell-shape changes in each process are often well understood, how these are driven mechanistically remains less clear. Most cell-shape changes require actin and myosin, and thus cytoskeletal regulatory proteins probably dictate the type of cell-shape change. Identifying how morphogenetic regulators work together will aid our understanding of how tissues and organs are shaped.

Drosophila embryogenesis is an attractive model in which to study morphogenesis. Many morphogenetic events have been characterized, which are likely to share mechanisms with vertebrate morphogenetic events. Through loss-of-function studies, mutants in which particular processes are affected have been identified. Mesoderm invagination in the ventral furrow (VF) is one such event (reviewed in Pilot and Lecuit, 2005). During gastrulation, a subset of ventral mesodermal precursor cells apically constrict in a highly coordinated fashion. This creates an invagination – the VF – which internalizes these cells as a tube; they then undergo an epithelial-mesenchymal transition. Internalization of VF cells also brings together two rows of mesectodermal cells of the CNS midline.

Genetic screens have identified two VF regulators that give insight into how the process works: the ligand Folded gastrulation (Fog) (Costa et al., 1994) and the G-α-protein Concertina (Cta) (Parks and Wieschaus, 1991). In either mutant, apical cell constriction occurs, but is uncoordinated, disrupting tube formation (Parks and Wieschaus, 1991; Sweeton et al., 1991). The mesodermal transcription factors Twist and Snail specify *fog* expression in the VF (Costa et al., 1994), and Fog acts upstream of Cta (Morize et al., 1998). The G-protein-coupled receptor for Fog remains unidentified.

Another VF regulator, the Rho1 activator RhoGEF2, provides a link between Fog-Cta signaling and the cytoskeleton (Hacker and Perrimon, 1998; Barrett et al., 1997). RhoGEF2, with a G-protein-interacting RGS domain, acts downstream of Cta in *Drosophila* embryos and cultured S2 cells (Rogers et al., 2004; Barrett et al., 1997). RhoGEF2 activates Rho1 to direct non-muscle myosin II (myosin) accumulation. Cta, Rho1 and RhoGEF2 are sufficient for myosin accumulation and cell constriction in S2 cells (Rogers et al., 2004), and loss of *fog*, *cta* or *RhoGEF2* disrupts apical myosin localization in the VF (Dawes-Hoang et al., 2005; Nikolaidou and Barrett, 2004).

These data provide an attractive model, but loss-of-function analysis suggests that unidentified players exist. *fog*- and *cta*-null mutants have uncoordinated cell constriction, but internalize mesoderm, albeit abnormally. By contrast, in *RhoGEF2*-null mutants, constriction fails entirely and mesoderm remains on the surface. This suggests that RhoGEF2 regulates apical constriction by both Cta-dependent and -independent mechanisms, but the Cta-independent mechanism remains mysterious.

Here we examine the role of Abelson (Abl) kinase in morphogenesis. Abl is unique among non-receptor tyrosine kinases, as it contains C-terminal actin-binding domains. Mammalian Abl regulates actin dynamics in cultured cells (reviewed in Woodring et al., 2003). Loss of both Abl and Abelson-related-gene (Arg, also known as Abl2 – Mouse Genome Informatics) during mouse development disrupts neural tube closure (Koleske et al., 1998). Neural tube closure mirrors VF formation, with apical cell constriction creating a tubular invagination that internalizes neurectoderm. Interestingly, Rho signaling also regulates this process (Brouns et al., 2000).

Drosophila Abl regulates both axon guidance and epithelial morphogenesis. In the CNS, Abl negatively regulates the actin modulator Enabled (Ena) (Gertler et al., 1995) by cooperating with other axon guidance regulators, including the Rho-family GEF Trio (reviewed in Lanier and Gertler, 2000). Loss of Abl disrupts actin organization in several epithelia, including in ovarian follicle cells (Baum and Perrimon, 2001) and in the embryonic epidermis during

[1]Department of Biology and [2]Lineberger Comprehensive Cancer Center, University of North Carolina at Chapel Hill, Chapel Hill, NC 27599-3280, USA.

*Author for correspondence (e-mail: peifer@unc.edu)

Accepted 20 November 2006

dorsal closure (Grevengoed et al., 2001). We examined the mechanism of action of Abl during the simpler stages of blastoderm development; there, Abl negatively regulates apical Ena localization in forming cells, thus regulating the location and type of actin polymerization. In *abl* mutants, actin accumulates in apical microvilli and is depleted from invaginating membrane furrows (Grevengoed et al., 2003).

Here, we describe a novel role for Abl in morphogenesis – that Abl regulates apical constriction of the VF. Our data further suggest a significant revision of the apical cell constriction model, helping explain phenotypic differences between *fog-cta* and *RhoGEF2*.

MATERIALS AND METHODS

Abl::GFP

The coding sequence of *abl* (cDNA GH09917; DGRC), without its stop codon, was fused 5′ of *egfp* and a 21-nucleotide linker (see Figs 2, 5). pUAS-Abl::GFP was cloned into pUASG. In the endogenous-Abl::GFP fusion construct, 2 kb 5′ of the *abl* start codon [BAC clone AC010688 (DGRC)] was introduced 5′ of the fusion and cloned into pUASG. Transgenics were produced by P-element transposition.

Fly stocks

Mutations were as described at http://flybase.bio.indiana.edu. $FRTRhoGEF2^{04291}$ was from U. Hacker (Lund University, Lund, Sweden) and cta^{RC10} from E. Wieschaus (Princeton University, Princeton, NJ, USA). *cta* embryos were from $cta^{RC10}/Df(2L)C'$ females. Germline clones used were as in Grevengoed et al. (Grevengoed et al., 2001). *cta;abl* embryos were from *hs-FLP/+;*cta^{RC10}*/Df(2L)C;FRT79D-Fabl*^{4}*,moesin::GFP/FRT79D-Fovo*^{D} mothers. All experiments were at 25°C. Live-imaging used moesin::GFP (Edwards et al., 1997).

S2 cells

Cell culture was as in Rogers et al. (Rogers et al., 2002); and RNAi as in Clemens et al. (Clemens et al., 2000). Double-stranded RNA-templates for in vitro transcription were generated by PCR introducing T7 promoters upstream of: *abl(–)* 5′-ACTGCATCTCCAGTTCCAGC-3′, 5′-ACTG-CATCTCCAGTTCCAGC-3′; control [pBluescriptSK(–)] 5′-TAAATTG-TAAGCGTTAATATTTTG-3′, 5′-GAATTCGATATCAAGCTTATCGAT-3′. For ransient transfections the Effectene kit (Qiagen) was used. Expression was driven by co-transfecting metallothionein-Gal4. DNAs used were UAS-cta^{R277H}Myc, UAS-rho^{V14} (S. Rogers, UNC-CH, Chapel Hill, NC, USA), and UAS-*abl::*GFP. The metallothionein promoter was induced with 500 μM $CuSO_4$ for 24 hours.

Immunofluorescence and immunoblotting

For fixation, the following were used: myosin, RhoGEF2, heat-methanol (Muller and Wieschaus, 1996); phalloidin/Ena 5 minutes, 37% formaldehyde; S2 cells, as in Rogers et al. (Rogers et al., 2004); all others, 20 minutes, 1:1 heptane:3.7% formaldehyde. Embryos were methanol- or hand-devitellinized (for phalloidin), blocked/stained in PBS/1% goat serum/0.1%TritonX-100. For antibodies/probes see Table 1. Embryo cross-sectioning was as in Dawes-Hoang et al. (Dawes-Hoang et al., 2005). Sample mounting was in Aqua-Polymount (Polysciences). For fixed sample imaging, Zeiss LSM510 or Pascal confocal microscopes and LSM software was used. When comparing the effects of Abl etc. on actin or myosin in S2 cells, all transfected cells within regions of the slide were analyzed. The LSM range-indicator feature was used on two control cells, and set such that the levels of actin or myosin in the control cells were just below saturation. Transfected cells were scored as increased if the range indicator said that they were above saturation. For live imaging, Perkin-Elmer UltraVIEW spinning-disc confocal, ORCA-ER digital camera, Metamorph software was used. All images were acquired at 40×. Adobe Photoshop7.0 was used to adjust brightness and contrast. When protein levels were compared, compared images were equally adjusted. Immunoblotting was carried out as in Grevengoed et al. (Grevengoed et al., 2001).

RESULTS

Abl regulates apical constriction

Abl regulates the type and location of actin polymerization in blastoderm embryos by regulating the localization of the actin regulator Ena (Grevengoed et al., 2003). Using this mechanistic insight, we revisited the roles of Abl in morphogenesis. Prior to morphogenesis, embryos that are maternally mutant for abl^{4}, a protein-null allele (see Fig. S1A in the supplementary material) (Bennett and Hoffmann, 1992), have cellularization defects. However, phenotypic severity varies with temperature: at 18°C embryos have many multinucleate cells, but at 25°C many embryos have few/no multinucleate cells (Grevengoed et al., 2003).

We took advantage of this to follow *abl* mutants with weak cellularization phenotypes into morphogenesis. *abl* mutants progress through morphogenesis relatively normally until germband retraction and dorsal closure, when obvious defects arise (Grevengoed et al., 2001). However, during this analysis, we uncovered a novel, fully penetrant phenotype earlier in development, during mesoderm invagination.

Table 1. Antibodies and probes

Antibody/probe	Dilution	Source
Anti-DE-CAD2	1:100	DSHB
Anti-Neurotactin	1:10	DSHB
Anti-β-PS1integrin	1:3	DSHB
Anti-Rho1	1:100	DSHB
Anti-Ena	1:200	DSHB
Anti-Myc	1:300	DSHB
Anti-ArmN2	1:200	DSHB
Anti-Twist	1:2000	S. Roth, University of Köln, Köln, Germany
Anti-Sim	1:50	S. Crews, UNC-CH, Chapel Hill, NC, USA
Anti-GFP	1:2000	Abcam
Anti-RhoGEF2	1:2000	S. Rogers, UNC-CH
Anti-Zipper (Myosin II heavy chain)	1:1250	C. Field, Harvard University, Boston, MA, USA
Anti-Phospho-Tyrosine	1:1000	Upstate Biotechnology
Anti-Phospho(Y412)-c-Abl	1:250	BioSource
Anti-Phospho-(Ser19)Myosin LC	1:200	Cell Signaling
Alexa-phalloidin	1:200	Molecular Probes
Secondary antibodies: Alexas 488, 568 and 647	1:500	Molecular Probes

DSHB, Developmental Studies Hybridoma Bank.

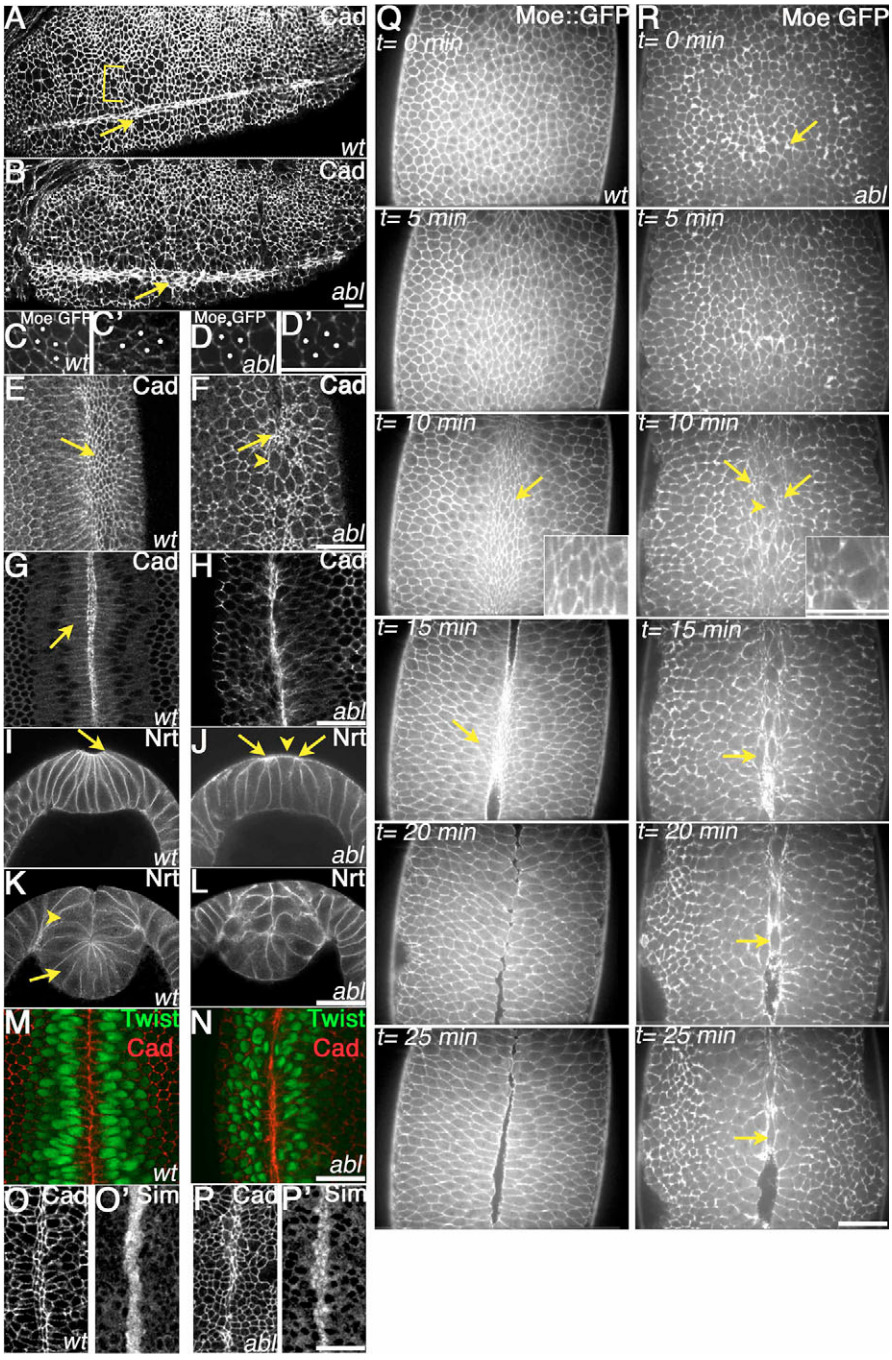

Fig. 1. Abl is required for coordinated apical constriction in the VF. Embryos, genotypes and antigens are indicated. (**A-D'**) Germband extension. (A,B) Dorsal view, anterior left; arrows indicate the ventral midline, bracket indicates the germband. (C-D') Living embryos. Moesin::GFP prior to (C,D) and after (C',D') cell intercalation. White dots highlight the rearrangement of cell contacts. (**E-H**) Grazing-sections, ventral. (E,F) Apical view of the VF at early gastrulation. (E) Arrow indicates uniform constriction in wild type. (F) *abl* mutant. Constricted (arrow) and unconstricted (arrowhead) cells are shown. (G,H) Subapical view at mid-gastrulation. (G) Arrow indicates lateral mesoderm orienting parallel to the VF. (H) *abl* mutant. Lateral mesoderm are pulled towards the VF at varying angles. (**I-L**) VF cross-sections. (I,J) Early gastrulation. (I) Wild type. Central cells constrict and point towards the furrow. Arrow indicates the outermost cells stretch over their neighbors. (J) *abl* mutant. Arrows indicate constricted cells; arrowhead indicates an unconstricted cell. (K,L) Late gastrulation. (K) Wild type. Arrow indicates wedge-shaped constricted cells; arrowhead indicates unconstricted lateral cells. (L) *abl* mutant. (**M**,**N**) Cad (red) and Twist (green) expression in wild-type (M) and *abl*-mutant (N) embryos in the late VF. (**O-P'**) Midline morphogenesis. (**Q**,**R**) Stills of living embryos expressing Moesin::GFP. (Q) Wild-type central cells constrict (*t*=10 minutes, arrow); lateral cells internalize without constriction (*t*=15 minutes, arrow). (R) *abl* mutant. At *t*=0 minutes, ectopic F-actin before VF formation (arrow) can be seen. At *t*=10 minutes, constricting cells (arrows) are interspersed with unconstricted cells (arrowhead). Inset in Q,R shows asymmetry in cell shape. At *t*=15, 20 and 25 minutes, mesodermal cells remain at the surface (arrows). Cad, DE-Cadherin; Nrt, Neurotactin; Sim, Single-minded; Moe::GFP, Moesin::GFP. Scale bar: 20 μm.

Gastrulation involves two main types of cell-shape change: apical constriction internalizes VF and posterior-midgut cells (Sweeton et al., 1991), and cell-cell intercalation extends the germband in the anterior-posterior axis (Irvine and Wieschaus, 1994). *abl* mutants showed no obvious germband extension defects (Fig. 1A vs 1B). To confirm that intercalation does not require Abl, we imaged live embryos expressing Moesin::GFP and therefore highlighting F-Actin (Edwards et al., 1997). The cell-cell contact rearrangements driving germband extension (Bertet et al., 2004) occurred normally in *abl* mutants (Fig. 1C vs 1D).

However, *abl* mutants displayed consistent ventral abnormalities (Fig. 1A vs 1B, arrows; Fig. 1O vs 1P). Because this phenotype is fully penetrant and only half of the embryos are both maternally and zygotically *abl* mutant, this phenotype appears to depend solely on maternal Abl. We thus investigated VF formation in *abl* mutants in detail. We were particularly interested in this process because it mimics neural tube closure, which fails in mice lacking both Abl and Arg (Koleske et al., 1998).

VF formation is triggered by regional expression of the Twist transcription factor, which specifies mesodermal fates and triggers morphogenesis. The first stage in VF formation is the apical constriction of individual cells scattered throughout the Twist-expressing domain (Sweeton et al., 1991). In wild-type fly embryos, central mesodermal precursors transition quickly from uncoordinated to coordinated constriction as the VF forms. We analyzed wild-type VF formation in detail in both fixed and living embryos. Central cells (Fig. 1E, arrow) apically constricted to a wedge shape (Fig. 1K, arrow), while more lateral VF cells (Fig. 1G,

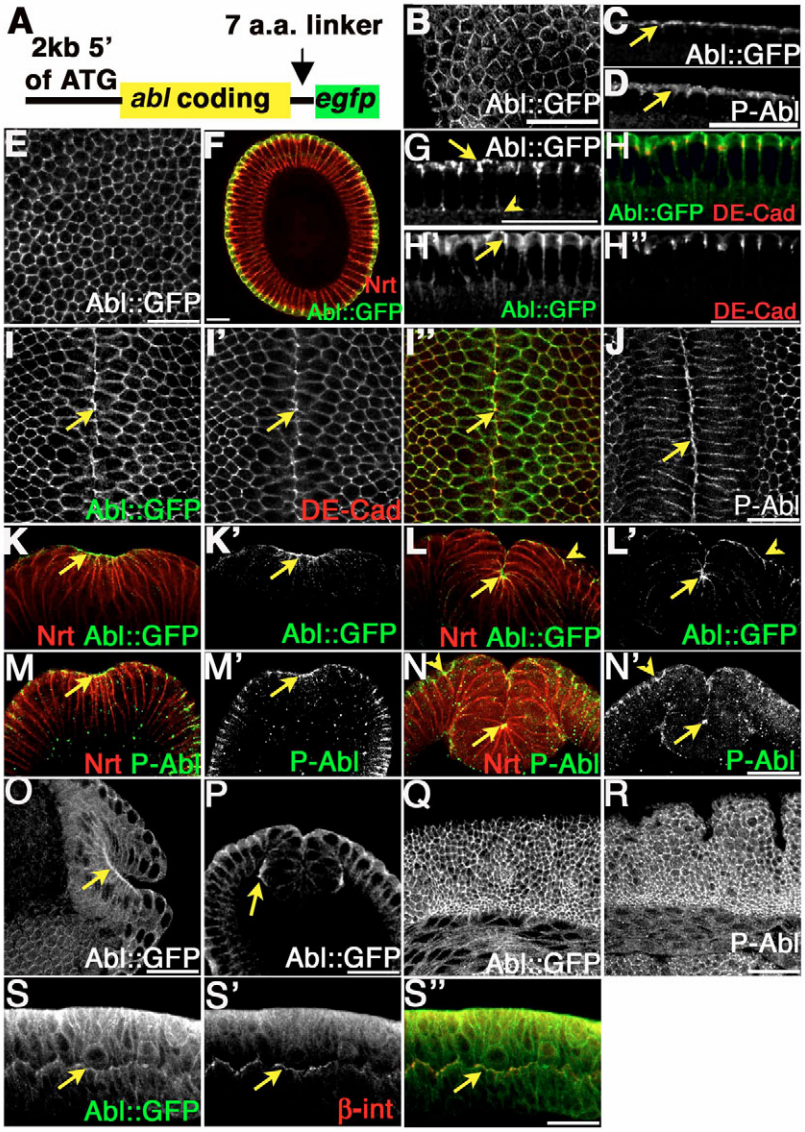

Fig. 2. Abl localization and activity. Wild-type or Abl::GFP embryos are shown. Antigens are indicated. (**A**) *abl::GFP* fusion construct. (**B-D**) Syncytial blastoderm. (B) Grazing-section. (C,D) Cross-sections showing apical Abl::GFP (C, arrow) and apical phosphorylated Abl (P-Abl; D, arrow). (**E-H″**) Cellularization. (E) Grazing-section. (F-H″) Cross-sections. (F) Abl::GFP localizes apically throughout (arrow). Nrt marks basolateral membranes. (G) Mid-cellularization; Abl::GFP is at high levels apically (arrow) and is at low levels in furrow canals (arrowhead). (H-H″) Late cellularization. Apical Abl::GFP (arrow) partially overlaps AJs (Cad). (**I-J**) Grazing-sections of the VF. Abl::GFP is elevated in the VF (arrows), overlapping constricting AJs (Cad). (J) P-Abl is elevated in the VF (arrow). (**K-N′**) Cross-sections of the VF. Abl::GFP (K,L) and P-Abl (M,N) concentrate in mesoderm in the early (K-K′) and late (L-L′) VF (arrows), and persist apically in non-mesoderm tissue (arrowheads; L,N). (**O**) Apical Abl::GFP in the posterior midgut (arrow). (**P**) Basal Abl::GFP localization (arrow) in the late VF. (**Q**,**R**) Germband-extension. Abl::GFP (Q) and P-Abl (R) at the cell cortex. (**S-S″**) Abl::GFP (S, green in S″) overlaps β-integrin (S′, red in S″) in ectoderm (arrows). P-Abl, Phospho-Abl; β-Int, β-PS-Integrin. Scale bar: 20 μm.

arrow) did not constrict but adopted an asymmetrical morphology, positioning their apices towards the invagination (Leptin and Grunewald, 1990) (Fig. 1K, arrowhead). Most remarkable were the outermost VF cells, which extended their apices far over neighboring cells towards the center of the VF (Fig. 1I, arrow). The difference in morphology between central constricting cells and more lateral cells probably reflects the lack of *fog* expression in lateral mesoderm (Costa et al., 1994).

abl mutants exhibited striking differences from wild type soon after the onset of VF formation. Whereas wild-type constriction was highly coordinated, apical constriction in *abl* mutants was not (Fig. 1F,H,J). Although some cells apically constricted, others remain unconstricted. In grazing sections, unconstricted cells appeared as large, rounded cells (Fig. 1F, arrowhead), probably stretched by the constriction of their neighboring cells (Fig. 1F, arrow). In cross-sections, instead of the central domain constricting to a common point, constricted cells (Fig. 1J, arrows) were interspersed with unconstricted cells (Fig. 1J, arrowhead). As VF formation continued, uncoordinated constriction altered VF cell shapes (Fig. 1K vs 1L) so that they pointed towards the furrow at varying angles (Fig. 1G vs 1H).

We first tested whether Abl is required for mesoderm specification, by examining expression of the mesodermal marker Twist. We observed no change in Twist expression in *abl* mutants (Fig. 1M vs 1N), and flanking mesectodermal cells continued to express Single-minded (a mesodermal marker; Fig. 1O′ vs 1P′), suggesting that cell fates were not altered.

We next examined VF formation live, examining how individual cell behaviors drive the overall process. This also allowed us to address a possible caveat not ruled out in our fixed-embryo analysis: that non-constricting cells in *abl* mutants could be multinucleate cells from earlier blastoderm defects. To ensure that multinucleate cells do not cause the *abl*-mutant defects, we only imaged embryos with few/no multinucleate cells (Fig. 1R, *t*=0 min) (Grevengoed et al., 2003). Wild-type mesodermal cells constricted uniformly and internalized synchronously. The difference between central and lateral cells of the furrow was evident; central cells uniformly constricted during internalization (Fig. 1Q, arrow, *t*=10 minutes; also see Movie 1 in the supplementary material); whereas lateral cells did not constrict, but elongated their apical ends towards the furrow during internalization (Fig. 1Q, arrow, *t*=15 minutes). By contrast, cell

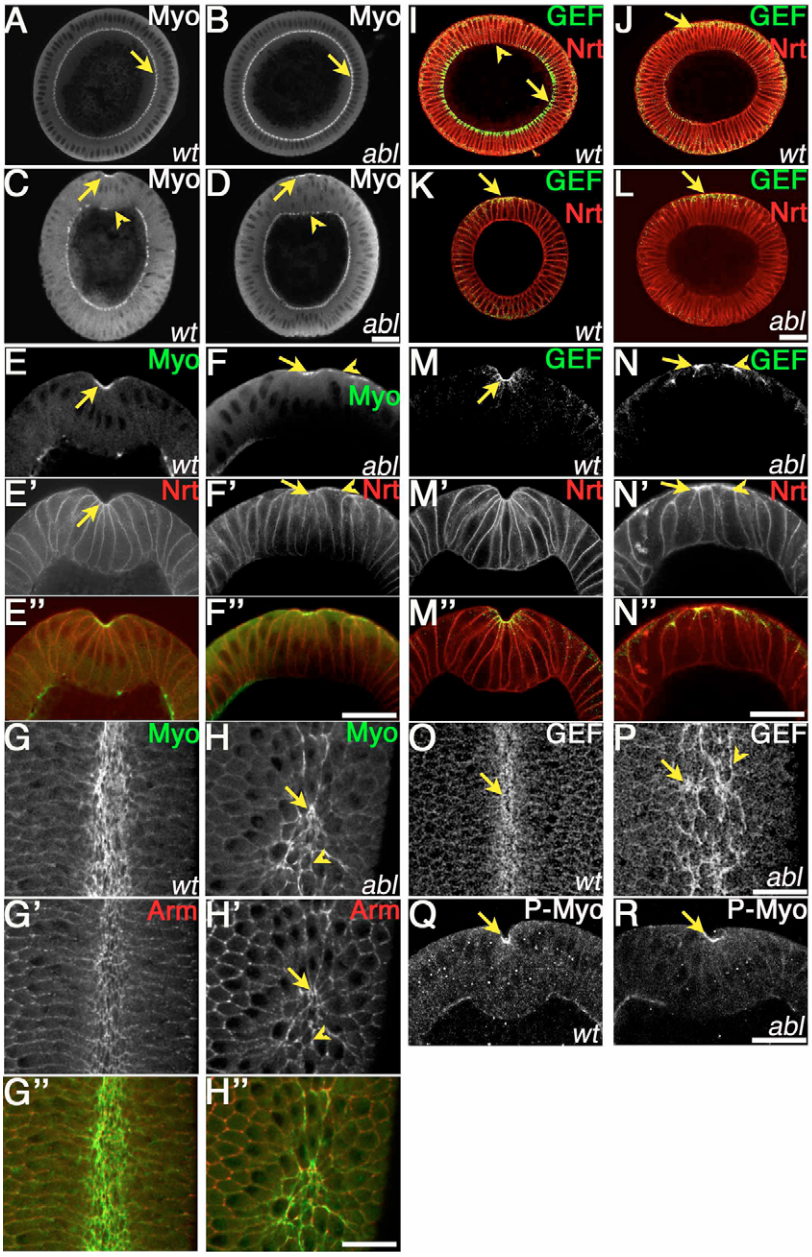

Fig. 3. Myosin and RhoGEF2 fail to uniformly assemble a contractile network in *abl* mutants. Embryos, antigens and genotypes are indicated. (**A-F″**) Cross-sections. (A-D) Low magnification. (A,B) Myosin in the basal furrow canals (arrows) in wild type (A) and *abl* mutants (B) at late cellularization. (C,D) Mesoderm in the early VF. Myosin disappears basally (arrowheads) and accumulates apically (arrows) in wild type (C) and *abl* mutants (D). (E-F″) Close-ups of the VF. (**G-H″**) Grazing-sections. (E-E″,G-G″) Myosin accumulates apically in wild-type constricting cells (arrow). (F-F″,H-H′) Myosin concentrates in constricting cells (arrows) in *abl* mutants, but is diffuse in unconstricting cells (arrowheads). (**I-N″**) Cross-sections taken at late cellularization-gastrulation onset. (I-K) Wild type. RhoGEF2 is lost basally in mesoderm (I, arrow vs arrowhead), and then accumulates apically (J,K, arrows). (L) *abl* mutant. RhoGEF2 accumulates apically (arrow). (M-N″) Cross-sections of the VF. (**O**,**P**) Grazing-sections of the VF. (M,O) In wild-type embryos, RhoGEF2 localizes strongly to all cells (arrows). (N,P) In *abl* mutants, RhoGEF2 localizes apically in constricting cells (arrows), but is diffuse in non-constricting cells (arrowheads). (**Q**,**R**) Cross-sections of the VF showing the expression of P-Myo by constant-level imaging. Similar levels of Myo-*P* (P-Myo) were observed at apical constriction sites (arrows) in wild type (Q) versus *abl* mutants (R). Myo, Myosin; GEF, RhoGEF2; Arm, Armadillo; P-Myo, Phospho-Myosin. Scale bar: 20 μm.

constriction in *abl* mutants was uncoordinated, and some cells never constricted. Defects arose when cell-shape changes initiated in the central, constricting cells (compare insets in Fig. 1Q vs 1R, *t*=5 and 10 minutes, respectively; also see Movie 2 in the supplementary material). When groups of neighboring cells constricted (Fig. 1R, *t*=10 minutes, arrows), they often appeared to pull non-constricting neighbors towards them (Fig. 1R, *t*=10 minutes, arrowhead), carrying them inside the embryo. Some unconstricted cells persisted on the surface after most cells internalized (Fig. 1R, *t*=15, 20 and 25 minutes, arrow). These cells may contribute to midline cell-shape irregularities in *abl* mutants (Fig. 1O vs 1P). However, most *abl* mutants eventually internalized all mesoderm, allowing the two rows of Single-minded-expressing midline cells to join (Fig. 1O′ vs 1P′). Despite defects in coordinated constriction, furrow formation in *abl* mutants occurred roughly as quickly as in wild type (Fig. 1Q vs 1R; also see Movies 1 vs 2 in the supplementary material).

Moesin::GFP also allowed us to visualize actin dynamics in *abl* mutants during VF formation. At the onset of apical constriction, ectopic apical actin patches were present (Fig. 1R, *t*=0 minutes, arrow), which were probably remnants of excess microvillar actin from cellularization (Grevengoed et al., 2003). Although these actin patches were common in *abl* mutants, they did not correlate with sites of failed constriction. We describe the contribution of actin localization to the VF phenotype in *abl* mutants in detail below. Overall, these results suggest that, during gastrulation, Abl regulates apical constriction in the VF but is dispensable for germband extension.

Abl localizes and is activated apically in embryonic epithelia

To better understand the mechanism of action of Abl during apical constriction, we investigated Abl localization. We took two approaches to examine Abl localization and to test the hypothesis

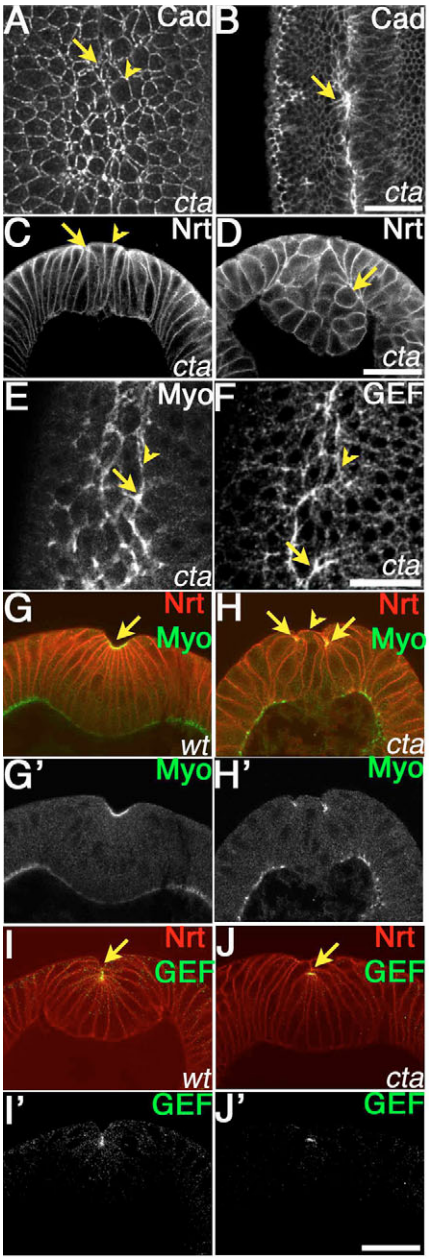

Fig. 4. *cta* mutants resemble *abl* mutants. Embryos, antigens and genotypes are indicated. (**A-F**) VFs from *cta* mutants. (A,B,E,F) Grazing-sections, (C,D,G-J′) Cross-sections. (A,C) Constricted (arrows) and unconstricted (arrowheads) cells at early gastrulation. (B,D) Late gastrulation. (B, arrow) Mesoderm internalized at varying angles. (D, arrow) Asymmetric cell shape. (E,F) During furrow ingression, apical myosin and RhoGEF2 are concentrated in constricting VF cells (arrows) and are diffusely localized elsewhere (arrowheads). (**G-J′**) Myosin and RhoGEF2 levels are comparable at sites of apical constriction (arrows) in wild type (G,I) and *cta* mutants (H,J), but, in the mutants, they are not concentrated in unconstricted cells (arrowheads). Scale bar: 20 μm.

that Abl is active apically. First, we added a C-terminal GFP-tag to Abl, joined by a linker peptide (Fig. 2A), as had been demonstrated to work with mammalian Arg::YFP (Wang et al., 2001). We cloned Abl::GFP downstream of 2 kb of the *abl* 5′ flanking sequence previously used in a rescuing transgene (Henkemeyer et al., 1987). Abl::GFP rescued *abl* mutants to viability and fertility (see Fig. S1B in the supplementary material), suggesting that it replicates endogenous Abl expression and localization. Second, we used a Phospho-specific antibody that recognizes a tyrosine in the activation loop that is phosphorylated during Abl activation. This tyrosine is conserved in *Drosophila* Abl, and the antibody recognizes active *Drosophila* Abl (T. Stevens, D.F. and M.P., unpublished data). Both reagents revealed a pool of Abl at the apical cortex of epithelial cells. We began analysis during the blastoderm stages, where we hypothesized Abl to act apically. Indeed, both Abl::GFP and phospho-Abl localized apically (Fig. 2C,D,F-H, arrows) and cortically (Fig. 2B,E). At mid-cellularization, some Abl also localized to basal furrow canals (Fig. 2G, arrowhead). Apical Abl overlapped adherens junctions (AJs), colocalizing with DE-Cadherin (Fig. 2H-H″), but also extended more apically, where other actin-associated proteins reside (Harris and Peifer, 2005).

Next, we examined Abl localization during gastrulation. As VF cells changed shape, both total (Fig. 2I,K,L) and active (Fig. 2J,M,N) Abl concentrated at sites of apical constriction (arrows). In non-mesodermal cells, lower levels of total and active Abl persisted apically (Fig. 2L,N, arrowheads). Abl was also enriched in apically constricting posterior midgut cells (Fig. 2O, arrow). Towards the end of VF formation, Abl also accumulated basally between the mesoderm and the neighboring ectoderm (Fig. 2P, arrow), perhaps in integrin-based contacts (Fig. 2S, arrows). Following gastrulation, Abl::GFP and phospho-Abl localized to apical junctions of all epithelial cells (Fig. 2Q,R). Thus, Abl localizes and is active apically, and its localization and activity concentrate at sites of apical constriction.

Apical myosin fails to uniformly contract in *abl* mutants

In embryos and S2 cells, RhoGEF2 promotes myosin organization into an apical contractile ring in constricting cells (Nikolaidou and Barrett, 2004; Rogers et al., 2004). To explore how Abl regulates apical constriction, we compared myosin and RhoGEF2 localization in wild-type and *abl*-mutant VFs. Myosin and RhoGEF2 largely colocalized in wild-type embryos. During cellularization, myosin and RhoGEF2 localized basally in furrow canals (Fig. 3A,I, arrows), as previously described (Dawes-Hoang et al., 2005; Grosshans et al., 2005; Padash Barmchi et al., 2005). Following cellularization, most cells retained myosin in basal yolk canals (remnants of cellularization contractile rings). However, mesodermal precursors strikingly relocalize myosin apically at, or immediately prior to, constriction (Nikolaidou and Barrett, 2004) (Fig. 3C,E,G, arrows). We also examined active myosin, using an antibody against the conserved myosin-light-chain Ser-19 phosphorylation site. Constricting cells exhibited elevated apical phosphorylated myosin (myosin-*P*) (Fig. 3Q, arrow). Unlike myosin, RhoGEF2 disappeared from basal furrow canals at the onset of gastrulation (Fig. 3J; this transition occurred slightly earlier in the mesoderm, Fig. 3I, arrowhead), exhibiting diffuse apical localization in all cells. Next, similar to myosin, RhoGEF2 accumulates at apical AJs of mesodermal precursors (Grosshans et al., 2005) (Fig. 3K, arrow). Apical RhoGEF2 was seen in cells before constriction (Fig. 3K), suggesting that, as with myosin (Nikolaidou and Barrett, 2004), apical RhoGEF2 precedes constriction. It was much easier to identify embryos with apical RhoGEF2 than apical myosin prior to constriction, suggesting that RhoGEF2 may precede myosin at AJs. RhoGEF2 localization during mesoderm internalization parallels myosin and Abl, concentrating at sites of apical constriction (Fig. 3M, arrow, O).

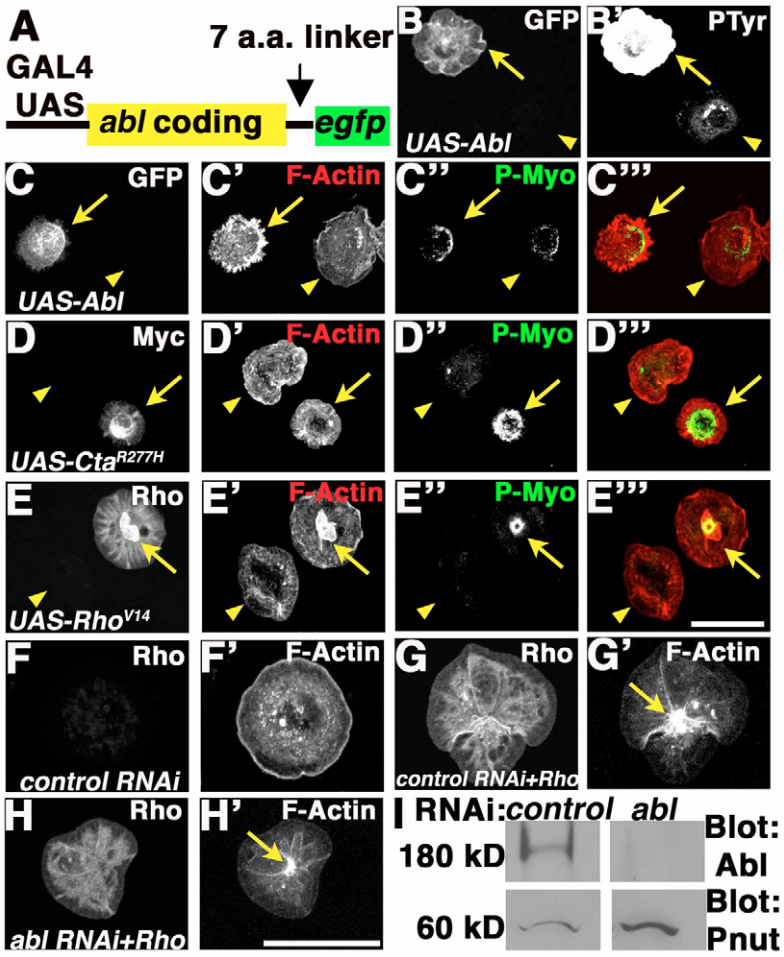

Fig. 5. In S2 cells, Abl promotes actin accumulation while Cta promotes myosin accumulation. S2 cells are shown, and the antigens, transfections and RNAi treatments are indicated. (**A**) UAS-Abl::GFP fusion construct. (**B-E‴**) Transfected cells. Arrows indicate UAS-Abl overexpressing cells in B,C; UAS-activated Cta in D; and UAS-activated Rho in E. Arrowheads indicate untransfected controls. Abl-transfected cells display elevated phosphorylated Tyr (P-Tyr; B′) and concentrated actin, but show no change in Myo-*P* (P-Myo) expression (C). (D) Cta-transfected cells display concentrated P-Myo, but not actin. (E) Rho-transfected cells exhibit concentrated actin and P-Myo, which are organized into a central ring. (**F-H′**) *abl* RNAi does not block Rho gain-of-function. (F) Control RNAi. (G,G′) Control RNAi+active Rho. Notice increased Rho and concentrated actin relative to F,F′. (H,H′) *abl* RNAi+active Rho. Rho and actin localization is similar to active Rho alone (G,G′). (**I**) Immunoblot showing knockdown of the Abl protein from the S2 cells shown in G-H′. Samples were non-adjacent on the same gel. Pnut, loading control; PTyr, Phospho-Tyrosine. Scale bar: 30 μm.

Many features of myosin and RhoGEF2 localization are normal in *abl* mutants, including basal myosin in furrow canals (Fig. 3B, arrow), and apical myosin and RhoGEF2 relocalization in mesodermal precursors (Fig. 3D,L, arrows). In cross-sections, constricting cells of *abl* mutants exhibited normal myosin and RhoGEF2 localization (Fig. 3F,N, arrows), and normal myosin-*P* levels (Fig. 3Q vs 3R, arrows). By contrast, however, in unconstricted cells of *abl* mutants, although the constriction machinery localized apically, it did not assemble into an effective contractile ring. In grazing sections, myosin and RhoGEF2 concentrated apically in constricting cells (Fig. 3H,P, arrows) but were diffuse and discontinuous in unconstricted cells (Fig. 3H,P, arrowheads); we saw similar results in cross-section (Fig. 3F,N, arrowheads). This *abl* phenotype contrasts with embryos lacking AJs, in which actomyosin rings constrict without constricting cells (Dawes-Hoang et al., 2005). Taken together, our results suggest that, in *abl* mutants, constriction machinery localizes apically but fails to constrict in some cells.

abl and *cta* mutants have similar effects on coordinated apical constriction

In *abl* mutants, VF cell constriction was uncoordinated, but mesodermal cells did internalize. This phenotype resembles that of *cta* and *fog* mutants (Parks and Wieschaus, 1991; Sweeton et al., 1991). To understand how Abl function relates to other VF regulators, we examined the *cta*-mutant phenotype in detail, revealing striking similarities between *abl* and *cta*, and new details about *cta* VF defects. *cta* mutants closely resemble *abl* mutants in VF cell morphology and phenotypic severity. In *cta* mutants, constricted cells appear next to unconstricted cells (Parks and Wieschaus, 1991) (Fig. 4A,C, arrows vs arrowheads), and mesodermal cells internalized at varying angles (Fig. 4B) and exhibited aberrant morphology after internalization (Fig. 4D, arrow).

We next examined the localization of the apical constriction machinery in *cta* mutants. Nikolaidou and Barrett (Nikolaidou and Barrett, 2004) reported lower levels of apical myosin in constricting cells in *cta* mutants than in wild type. However, when we compared wild-type and mutant embryos stained and imaged together, we saw no decrease in apical myosin in constricting cells (Fig. 4G vs 4H, arrows). We did, however, find sections with little or no apical myosin, which represent sections through few or no constricting cells. Myosin failed to assemble into continuous contractile structures in unconstricted cells of *cta* mutants (Fig. 4E), as in *abl* mutants. RhoGEF2 localization was non-uniform in the VF, concentrating where cells successfully constricted (Fig. 4F, arrows in 4I vs 4J), as in *abl* mutants, consistent with the idea that defects in RhoGEF2 localization in *cta* mutants disrupt myosin activation. Thus, both *abl* and *cta* mutants have unconstricted cells where RhoGEF2 and myosin fail to assemble a contractile network.

In S2 cells Abl regulates actin while Cta regulates myosin

Our data suggest that both Abl and Cta promote actomyosin-based contraction during VF formation. To better understand the mechanisms by which they function, we used a single-cell assay for

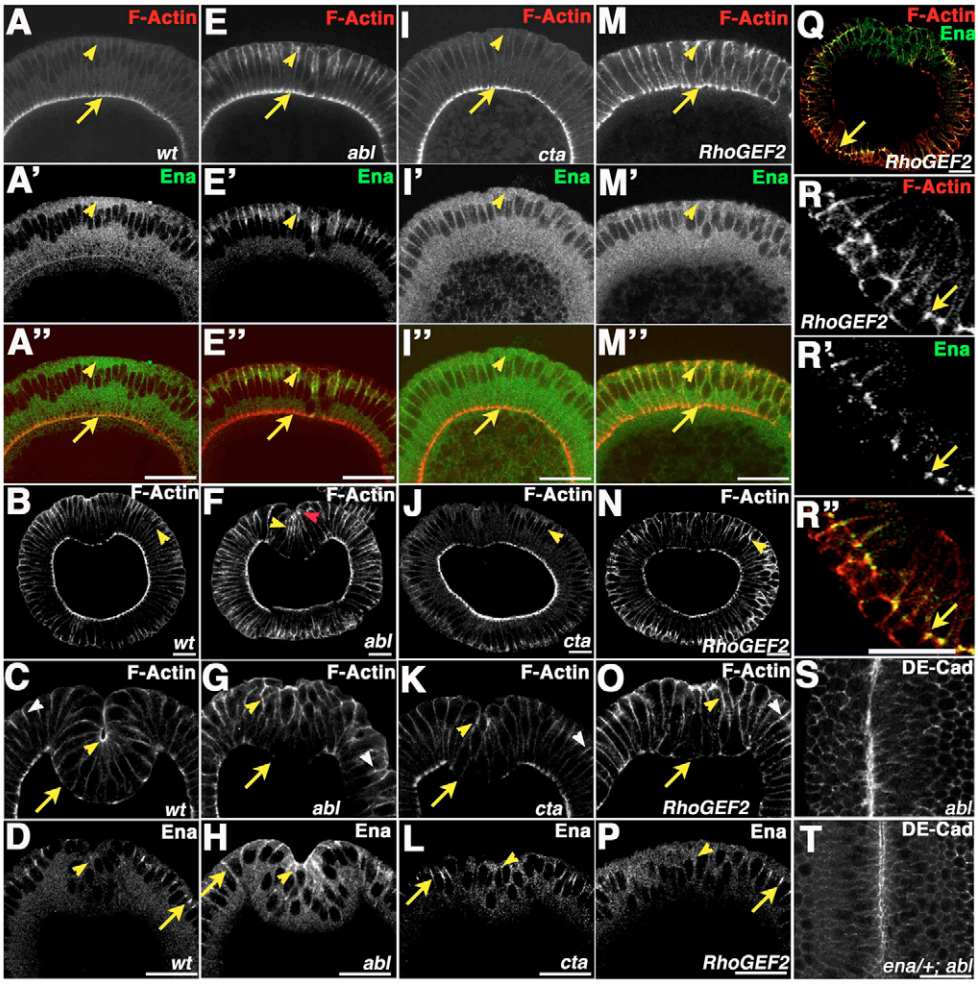

Fig. 6. Actin localization is altered in *abl* and *RhoGEF2*, but not in *cta*, mutants. Embryos and antigens are indicated. (**A-D**) Wild type; (**E-H**) *abl* mutant; (**I-L**) *cta* mutant; (**M-P**) *RhoGEF2* mutant. (A,E,I,M) Late cellularization. Actin is localized basally in all genotypes (arrows), but also accumulates apically (arrowheads) in *abl* (E) and *RhoGEF2* (M) mutants. Ena is diffusely localized in wild-type (A′), and in *cta* (I′) and *RhoGEF2* (M′) mutants, but accumulates apically in *abl* mutants (E′, arrowheads). (B,F,J,N) VF initiation. Ectopic apicolateral actin localization (arrowheads) occurs in *abl* (F) and *RhoGEF2* (N) mutants, but not in wild-type (B) or *cta* mutants (J). (F) Red arrowhead shows accumulated actin in constricting cells. (C,G,K,O) Close-up of the VF. (C) Wild-type. Actin is at apical AJs in most cells (white arrowhead). In the mesoderm, actin accumulates apically in constricting cells (yellow arrowhead), and disappears basally (arrow). (G) *abl* mutant. Ectopic actin in apically-constricting cells (yellow arrowhead) and non-constricting cells (white arrowhead). Arrow indicates the disappearance of normal basal actin. (K) *cta* mutant. Actin localization is normal (arrow, arrowheads as in C). (O) *RhoGEF2* mutant. Actin defects resemble those in *abl* mutants. Arrows and arrowheads are as in G. (D,H,L,P) Close-up of the VF. Arrows indicate non-mesodermal Ena. (D) Wild type. Ena concentrates at AJs in non-mesodermal cells, but remains diffuse in mesodermal cells (arrowhead). (H) *abl* mutant. Ena accumulates apicolaterally in non-mesodermal (arrow) and mesodermal (arrowhead) cells. (L,P) Neither *cta* (L) nor *RhoGEF2* (P) mutants accumulate ectopic mesodermal Ena (arrowhead). (**Q-R″**) *RhoGEF2* mutant at late gastrulation. In non-mesodermal cells, excess apical actin colocalizes with Ena in ectopic structures (arrows). (R) Close-up of Q. (**S**,**T**) *ena* heterozygosity suppresses the VF phenotype of *abl* mutants. (S) *abl* mutant. (T) *ena/+;abl* embryo. Scale bar: 20 μm.

actin and myosin organization during cell constriction in *Drosophila* S2 cells. Overexpression of RhoGEF2-pathway components, including activated Cta or Rho, promotes myosin reorganization in S2 cells (Rogers et al., 2004). Constitutively active Rho^{V14} also promotes actin organization (S. Rogers, personal communication). We thus examined both myosin and actin localization in S2 cells in response to Abl (using UAS-Abl::GFP, Fig. 5A), Cta and Rho overexpression. We also used RNAi loss-of-function to test whether Abl can function in the RhoGEF2 pathway.

Expression of Abl in S2 cells elevated tyrosine-kinase activity, as assessed by Phospho-Tyrosine levels (Fig. 5B,B′). In approximately 50% of these cells, morphology changed from a smooth peripheral edge to one with numerous projections (Fig. 5C′, arrow). Furthermore, UAS-Abl cells had elevated peripheral actin (Fig. 5C′, 23/50 cells examined; in this and similar comparisons, the LSM range indicator was used to compare actin or myosin levels in randomly selected transfected cells to two control cells, see Materials and methods for details). By contrast, UAS-Abl cells exhibited normal myosin-*P* localization (45/50 cells, Fig. 5C″). Activation of Cta in S2 cells had strikingly different effects from Abl-overexpression. myosin-*P* was locally elevated in a ring-like structure in response to constitutively active Cta::Myc^{R277H} (Morize et al., 1998) (Fig. 5D″, arrow, 30/50 cells). By contrast, these cells did not exhibit consistent changes in actin organization, either in the cell periphery, as seen for Abl, or in a ring-like structure, as described below for Rho (Fig. 5D′, absent in 43/50 cells). Thus, in S2 cells Abl and Cta promote actin and myosin organization, respectively.

Overexpression of Rho^{V14} altered both actin (Fig. 5E′, 37/50 cells) and myosin-*P* localization (Fig. 5E″, 49/50 cells). In contrast to UAS-Abl cells, actin in Rho^{V14} cells localized to a ring above the cell center that colocalizes with myosin (arrows in Fig. 5E′-E‴). Myosin localization in Rho^{V14} cells differed qualitatively from most Cta^{R277H} cells, forming a tighter ring (Fig. 5E″ vs 5D″), as was previously observed (Rogers et al., 2004). Thus, Rho overexpression combines elements of both Abl and Cta overexpression, concentrating both actin and myosin-*P* into a ring-like contractile structure.

We next asked whether Abl is required for the gain-of-function phenotype of Rho by performing *abl* RNAi in Rho^{V14} S2 cells. Loss of Abl had no obvious effects on F-actin in wild-type S2 cells (data not shown) (Rogers et al., 2003). Despite efficient Abl knockdown

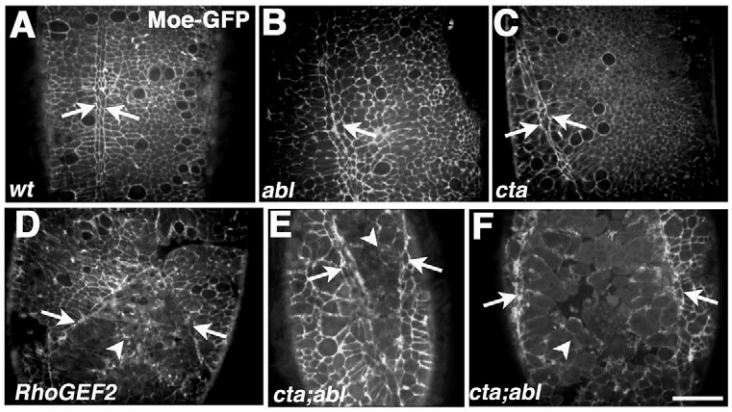

Fig. 7. *cta;abl* double mutants resemble *RhoGEF2* mutants. Moesin::GFP. (**A**) Wild type; (**B**) *abl* mutant; (**C**) *cta* mutant. (A-C) Mesoderm is internalized and midline cells meet (arrows). (**D**) *RhoGEF2* mutant; (**E**,**F**) *cta;abl* double mutant. Mesoderm is not internalized (arrowhead) and midline cells do not meet (arrows). Scale bar: 20 μm.

(Fig. 5I), the Rho^{V14} phenotype was unaffected by *abl* RNAi (arrows in Fig. 5G′ vs 5H′). This suggests that Abl does not act downstream of Rho signaling in S2 cells.

Abl regulates actin via the downregulation of Ena in the ventral furrow

Our results from overexpression of Abl in S2 cells together with work on the protein as an actin regulator in flies and mammals suggested that Abl might regulate VF apical constriction via actin. To test this mechanistic hypothesis, we examined actin regulation in the VF. At the end of cellularization, actin localized predominantly to basal furrow canals (Fig. 6A, arrow). During VF formation, actin was also found apically, forming a broad band in non-mesodermal cells (Fig. 6C, white arrowhead), and focusing to a tight band in VF cells (Fig. 6C, yellow arrowhead); actin also disappeared basally in only VF cells (Fig. 6B,C, arrow). This parallels myosin localization changes (Fig. 3). Thus, actin is highly polarized during cell constriction, being restricted to a tight ring at apical AJs.

One key Abl target in other contexts is the actin regulator Ena. We next examined whether Ena activity is regulated during VF formation and whether this is crucial for apical constriction. Prior to apical constriction, Ena localized diffusely (Fig. 6A′, arrowhead), but, during VF formation, it exhibited a striking difference in localization between mesoderm and non-mesoderm, concentrating at apical AJs in non-mesodermal cells (Fig. 6D, arrow). However, Ena remained noticeably absent in VF cells as apical constriction initiates (Fig. 6D, arrowhead), suggesting that it is downregulated in these cells. Thus, actin and Ena show opposite changes in localization in VFs.

Abl can regulate both Ena and actin, and we thus tested the hypothesis that Abl regulates these changes in actin and Ena localization. In cellularizing *abl* mutants, actin and Ena accumulated ectopically along the apicolateral membrane (Fig. 6E,E′, arrowheads; Fig. 1R, *t*=0 minutes, arrow). During VF formation, actin reorganization in the mesoderm failed in *abl* mutants. In wild type, actin was tightly focused to the apex of constricting cells (Fig. 6C, yellow arrowhead), while it localized to a broader band in non-mesodermal cells (white arrowhead). By contrast, in *abl* mutants, actin was found all along the apicolateral membrane of mesodermal cells (Fig. 6F,G, yellow arrowheads). However, cells that successfully constricted accumulated elevated apical actin (Fig. 6F, red arrowhead).

The normal downregulation of cortical Ena observed in wild-type mesoderm did not occur in *abl* mutants. Instead, Ena accumulated at high levels at the apicolateral cortex of mesodermal cells (Fig. 6H, arrowhead; ectopic Ena also accumulated apicolaterally in non-mesodermal cells). Thus, Abl is essential for the downregulation of Ena in VF cells, and this appears essential for the correct organization of apical actin in constricting cells.

To test the hypothesis that Ena-deregulation underlies actin and apical constriction defects in *abl* mutants, we genetically reduced Ena levels in *abl* mutants and asked if this rescued the VF phenotype of *abl* mutants. In embryos from maternally ena^{210}/+; *abl* females, the VF phenotype was largely suppressed (normal VF in 14/16 examined; Fig. 6S vs 6T). Together, these results suggest that Abl-dependent Ena-downregulation in VF cells is essential for ordered apical actin assembly and coordinated cell constriction.

RhoGEF2, but not Cta, regulates ventral furrow actin localization

These results suggest that, in addition to myosin regulation, organization of the actin network is a key mechanistic input into ordered apical constriction. We next asked whether other VF regulators also direct actin localization, examining actin and Ena localization in *cta* and *RhoGEF2* mutants. As actin localization defects arise prior to gastrulation in *abl* mutants (Grevengoed et al., 2003), we examined both cellularization and gastrulation. *cta* mutants showed no obvious actin localization defects during either cellularization (Fig. 6I) or gastrulation (Fig. 6J,K), paralleling our results in S2 cells, where Cta activation did not effect actin localization (Fig. 5). Furthermore, Ena downregulation occured normally in *cta* mutants (Fig. 6I′,L, arrowhead vs arrow). Thus, although *abl* and *cta* mutants have similar VF phenotypes, they appear to regulate this process via distinct mechanisms.

In contrast to *cta* mutants, *RhoGEF2* mutants display actin mis-localization very similar to that of *abl* mutants. During cellularization, actin accumulates ectopically in apicolateral regions (Padash Barmchi et al., 2005) (Fig. 6M, arrowhead), as in *abl* mutants. This actin localization defect persisted in all cells during VF formation (Fig. 6N,O), similar to *abl*. Excess actin accumulated along apicolateral membranes (Fig. 6N,O, yellow arrowhead), resulting in a less-focused actin network (Fig. 6O). However, Ena did not accumulate apically during either cellularization (Fig. 6M′) or VF formation (Fig. 6P), thus differing from *abl* (in later *RhoGEF2* mutants, actin and Ena did co-localize outside the mesoderm to a distinct apical domain; Fig. 6Q-R″, arrows). Thus, both Abl and RhoGEF2 are essential for proper apical actin organization prior to and during VF formation. Whereas Abl acts via Ena, RhoGEF2 appears to act via a distinct mechanism.

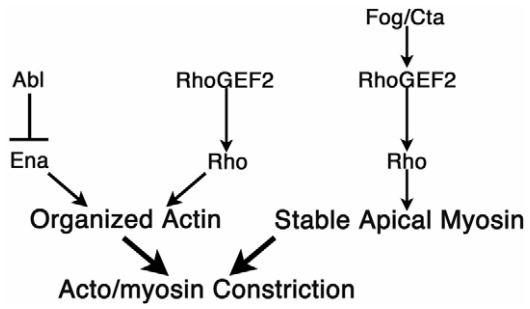

Fig. 8. A mechanistic model of ventral furrow formation.

Abl and Cta work in parallel to promote ventral furrow formation

Our results suggest that the assembly of an apically polarized actin network is a key mechanistic input into apical constriction. Further, the normal actin localization in *cta* mutants suggests that actin organization is independent of Fog-Cta signaling. This led us to ask whether the role of RhoGEF2 in actin organization could account for the difference in VF phenotypes between *cta* and *RhoGEF2* mutants. To examine this mechanistic model, we disrupted both actin organization and Fog-Cta signaling, the two cues lacking in *RhoGEF2* mutants, by generating *cta;abl* double mutants. We compared their phenotype to *RhoGEF2* mutants. In *RhoGEF2* mutants, the two lateral rows of midline cells fail to join (Fig. 7A vs 7D, arrows), due to failure of mesoderm internalization (Fig. 7D, arrowhead). This was not seen in either *cta* or *abl* single mutants (Fig. 7B,C). However, *cta;abl* mutants phenocopy *RhoGEF2* mutants. In double mutants, mesoderm remains on the surface (Fig. 7E,F, arrowheads) and midline cells do not join, a phenotype that was never observed in either single mutant (Fig. 7E,F arrows). Thus, both apical actin organization and Fog-Cta signaling appear to be key mechanistic inputs into mesoderm internalization.

DISCUSSION

Regulation of apical constriction during *Drosophila* VF formation is a paradigm for how signal transduction directs morphogenesis. Here, we identify Abl as a novel regulator of this process. Our results suggest that Abl acts in parallel to the known signaling pathway that promotes apical myosin activation by helping to organize a continuous apical actin network. Furthermore, our results help to explain the greater severity of the *RhoGEF2*-mutant phenotype relative to other VF mutants by suggesting that RhoGEF2 plays crucial roles in both myosin and actin regulation.

A mechanistic model of apical cell constriction

Previous work established myosin as a key output of RhoGEF2 signaling during mesoderm internalization (Dawes-Hoang et al., 2005; Nikolaidou and Barrett, 2004; Rogers et al., 2004). However, ambiguities remained regarding the circuitry of this pathway, as the *RhoGEF2* phenotype is much more severe than that of *cta* or *fog* mutants, suggesting that a simple linear pathway is unlikely. Our data suggest that RhoGEF2 plays dual roles in actin and myosin regulation, and thus its inactivation has more severe effects.

From our data, we developed a mechanistic model for the regulation of apical constriction during VF formation (Fig. 8). The regulation of actin localization by Abl and RhoGEF2 promotes organization of the apical actin network in constricting cells. We suggest that Abl regulates actin by actively downregulating cortical Ena in mesoderm, thus leading to polarized actin accumulation, similar to the role that it was shown to play in follicle cells (Baum and Perrimon, 2001). RhoGEF2 plays a distinct, Cta-independent role in the effective assembly of organized apical actin. While RhoGEF2 and Abl are modulating actin assembly, the mesodermal transcription machinery activates Fog-Cta signaling (Costa et al., 1994), apically stabilizing RhoGEF2. This allows the efficient activation of apical myosin. Coupling of these two cues – an organized apical actin ring at AJs and stable apical myosin activation – cooperate to ensure highly coordinated actomyosin constriction throughout the sheet of mesodermal cells in a short timeframe.

This model helps explain the mutant phenotypes observed in this and previous studies. In *abl* mutants, Fog-Cta allow RhoGEF2 stabilization and myosin contraction, but the lack of organized mesodermal actin in these mutants (Fig. 6F), which results from inappropriate Ena regulation (Fig. 6H,T), prevents the uniform assembly of actin-based contractile rings. *cta* mutants lack a stabilizing signal for RhoGEF2, preventing uniform apical myosin activation (Dawes-Hoang et al., 2005; Nikolaidou and Barrett, 2004) and uniform constriction. However, some cells can constrict without Fog-Cta (Sweeton et al., 1991), accumulating apical myosin levels comparable to those in wild type (Fig. 4H). In *RhoGEF2* mutants, the combined failure to stabilize/activate myosin (Dawes-Hoang et al., 2005; Nikolaidou and Barrett, 2004) and a lack of organized apical actin (Fig. 6N) severely compromises apical constriction. The similarity between *RhoGEF2* and *cta;abl* mutants supports this model, as both processes should be compromised.

Actin regulation during mesoderm internalization

Our model suggests that organized apical actin is an essential prerequisite for cell constriction. Although both Abl and RhoGEF2 regulate actin localization, our data argue that each acts independently. First, actin defects arise during cellularization, when Abl and RhoGEF2 have non-overlapping localizations (Fig. 2H vs Fig. 3I). Second, whereas Abl clearly acts through Ena, loss of RhoGEF2 disrupts actin without altering Ena localization (Fig. 6M′). Finally, Abl is not a Rho effector in S2 cells (Fig. 5H).

Several unanswered questions remain. With respect to *abl*, a major question is why do some cells apically constrict while others fail? This phenotype resembles the cellularization defects of *abl* mutants (Grevengoed et al., 2003), in which only some cells fail to reorganize actin into furrows. However, all cells exhibit excess apical Ena and thus form abnormally long, apical microvilli. Perhaps, in some cells, furrow actin assembly drops below a crucial threshold and furrows fail. In the VF, the absence of Abl may have similar effects. VF defects could result from both competition for cellular actin and recruitment of other regulators (e.g. the formin Diaphanous) to ectopic locations, preventing their action in VF formation. This may reduce actin assembly into contractile rings. When constriction initiates, stochastic variations in ring strength may lead some rings to fail, leading to unconstricted cells. Future work is needed to identify the full set of actin regulators involved, and to assess how they work. Interestingly, recent work implicates Abl in epithelial-mesenchymal transitions (Yang et al., 2006). Whereas Abl disrupts VF formation, Twist is normally localized in *abl* mutants (Fig. 1M,N), suggesting that this major regulator of such transitions is not an Abl target in flies.

Our data also reveal the importance of mesodermal Ena downregulation. This may result from increased mesodermal Abl activity, suggested by elevated levels of mesodermal Abl relative to non-mesoderm; however, this remains to be tested. We also need to identify the mechanism by which Abl regulates Ena. In some places,

such as the syncytial blastoderm, Abl localizes to sites where Ena is normally absent and, in the absence of Abl, ectopic Ena is found at these sites. This suggests that Abl actively antagonizes Ena localization. At other times and regions, however, such as the leading-edge during dorsal closure, Abl co-localizes with Ena, and thus may hold it in an inactive state. In VFs, Abl localizes to the apical-lateral cortex, and Ena localizes to this site in its absence. Further studies of Abl action will be needed to clarify the mechanisms by which it downregulates Ena.

Interestingly, manipulating mammalian Ena/VASP can affect cell contractility (Galler et al., 2006; Hoffman et al., 2006). Thus, Ena-downregulation may permit proper VF cell contractility. Testing this hypothesis will be important.

Our results also raise questions regarding RhoGEF2. Our model suggests that RhoGEF2 acts via two mechanisms, only one of which is Cta-dependent. Perhaps another upstream cue acts on RhoGEF2 to promote actin organization. Because *RhoGEF2* mutants have actin-organization defects in all cells, this regulator may act in all cells prior to gastrulation. However, our data do not rule out a second mesoderm-specific RhoGEF2 regulator acting in parallel to Cta (see Note added in proof). Although Rho-Kinase is a potential Rho effector with respect to myosin (Dawes-Hoang et al., 2005; Rogers et al., 2004), another effector may regulate actin organization. Attractive candidates are the Formins, which reorganize actin in many processes (Faix and Grosse, 2006).

Abl is required for specific cell-shape changes

Our data strengthen the idea that different cytoskeletal regulators direct distinct morphogenetic processes. Both Abl (our data) and Fog (Sweeton et al., 1991; Bertet et al., 2004) regulate mesodermal apical constriction but are dispensable for germband cell-cell intercalation. Thus, although both processes require dynamic myosin reorganization (Nikolaidou and Barrett, 2004; Zallen and Wieschaus, 2004), distinct regulators act in each.

The picture becomes more complex when considering other roles of Fog, Cta and RhoGEF2. All are required for internalization of the posterior midgut and salivary glands (Nikolaidou and Barrett, 2004; Barrett et al., 1997; Sweeton et al., 1991), but these cells internalize in *abl* mutants (data not shown). Thus, different types of apical constriction may be regulated differently. It will be interesting to explore the roles of Fog, Cta and RhoGEF2 during dorsal closure, which requires Abl.

Conserved roles for Abl and Rho during apical constriction

Our work supports mechanistic connections between VF formation and neural tube closure. Both involve actin-based apical constriction to internalize a sheet of cells into a tube. Mice lacking Abl and Arg kinases have neural tube defects, and actin organization in neuroepithelial cells appears altered (Koleske et al., 1998); interestingly, these cells have ectopic actin that is less polarized than normal, similar to what we observed in *abl*-mutant VFs. Furthermore, double-mutant analysis suggests that mammalian Ena plays a role in neural tube closure in conjunction with Profilin (Lanier et al., 1999). Thus, Abl-Ena signaling may represent a conserved mechanism of actin regulation during apical constriction. Our mechanistic insights can now be pursued in mammals.

Rho also regulates neural tube closure. Mice lacking p190RhoGAP have neural tube defects (Brouns et al., 2000). Interestingly, p190RhoGAP is an Arg substrate in the brain (Hernandez et al., 2004), suggesting possible direct links between Abl and Rho in apical constriction. The role of *Drosophila* p190RhoGAP in the VF has yet to be examined, but RhoGAP68F is implicated in VF formation (Sanny et al., 2006). Future work in both flies and mice will provide further mechanistic insights into conserved mechanisms of apical cell constriction.

We thank A. Koleske, G. Rogers and S. Rogers for advice; G. Bain, M. Cooper and F. Wang for technical assistance; S. Crews, C. Field, F. Fogerty, U. Hacker, R. Karess, D. Kiehart, S. Rogers, S. Roth and E. Wieschaus for reagents; and B. Goldstein, S. Rogers and J. Sawyer for discussions. This work was supported by NIHRO1GM47857.

Supplementary material

Supplementary material for this article is available at
http://dev.biologists.org/cgi/content/full/134/3/567/DC1

Note added in proof

We highlighted the potential for a second mesoderm-specific RhoGEF2 regulator that acts in parallel to Cta in this paper. Since submission of this manuscript, Kölsch et al. (Kölsch et al., 2007) have identified such a regulator – a transmembrane protein that can bind RhoGEF2.

References

Barrett, K., Leptin, M. and Settleman, J. (1997). The Rho GTPase and a putative RhoGEF mediate a signaling pathway for the cell shape changes in Drosophila gastrulation. *Cell* **91**, 905-915.

Baum, B. and Perrimon, N. (2001). Spatial control of the actin cytoskeleton in Drosophila epithelial cells. *Nat. Cell Biol.* **3**, 883-890.

Bennett, R. L. and Hoffmann, F. M. (1992). Increased levels of the Drosophila Abelson tyrosine kinase in nerves and muscles: subcellular localization and mutant phenotypes imply a role in cell-cell interactions. *Development* **116**, 953-966.

Bertet, C., Sulak, L. and Lecuit, T. (2004). Myosin-dependent junction remodelling controls planar cell intercalation and axis elongation. *Nature* **429**, 667-671.

Brouns, M. R., Matheson, S. F., Hu, K. Q., Delalle, I., Caviness, V. S., Silver, J., Bronson, R. T. and Settleman, J. (2000). The adhesion signaling molecule p190 RhoGAP is required for morphogenetic processes in neural development. *Development* **127**, 4891-4903.

Clemens, J. C., Worby, C. A., Simonson-Leff, N., Muda, M., Maehama, T., Hemmings, B. A. and Dixon, J. E. (2000). Use of double-stranded RNA interference in Drosophila cell lines to dissect signal transduction pathways. *Proc. Natl. Acad. Sci. USA* **97**, 6499-6503.

Costa, M., Wilson, E. T. and Wieschaus, E. (1994). A putative cell signal encoded by the folded gastrulation gene coordinates cell shape changes during Drosophila gastrulation. *Cell* **76**, 1075-1089.

Dawes-Hoang, R. E., Parmar, K. M., Christiansen, A. E., Phelps, C. B., Brand, A. H. and Wieschaus, E. F. (2005). folded gastrulation, cell shape change and the control of myosin localization. *Development* **132**, 4165-4178.

Edwards, K. A., Demsky, M., Montague, R. A., Weymouth, N. and Kiehart, D. P. (1997). GFP-moesin illuminates actin cytoskeleton dynamics in living tissue and demonstrates cell shape changes during morphogenesis in Drosophila. *Dev. Biol.* **191**, 103-117.

Faix, J. and Grosse, R. (2006). Staying in shape with formins. *Dev. Cell* **10**, 693-706.

Galler, A. B., Garcia Arguinzonis, M. I., Baumgartner, W., Kuhn, M., Smolenski, A., Simm, A. and Reinhard, M. (2006). VASP-dependent regulation of actin cytoskeleton rigidity, cell adhesion, and detachment. *Histochem. Cell Biol.* **125**, 457-474.

Gertler, F. B., Comer, A. R., Juang, J. L., Ahern, S. M., Clark, M. J., Liebl, E. C. and Hoffmann, F. M. (1995). enabled, a dosage-sensitive suppressor of mutations in the Drosophila Abl tyrosine kinase, encodes an Abl substrate with SH3 domain-binding properties. *Genes Dev.* **9**, 521-533.

Grevengoed, E. E., Loureiro, J. J., Jesse, T. L. and Peifer, M. (2001). Abelson kinase regulates epithelial morphogenesis in Drosophila. *J. Cell Biol.* **155**, 1185-1198.

Grevengoed, E. E., Fox, D. T., Gates, J. and Peifer, M. (2003). Balancing different types of actin polymerization at distinct sites: roles for Abelson kinase and Enabled. *J. Cell Biol.* **163**, 1267-1279.

Grosshans, J., Wenzl, C., Herz, H. M., Bartoszewski, S., Schnorrer, F., Vogt, N., Schwarz, H. and Muller, H. A. (2005). RhoGEF2 and the formin Dia control the formation of the furrow canal by directed actin assembly during Drosophila cellularisation. *Development* **132**, 1009-1020.

Hacker, U. and Perrimon, N. (1998). DRhoGEF2 encodes a member of the Dbl family of oncogenes and controls cell shape changes during gastrulation in Drosophila. *Genes Dev.* **12**, 274-284.

Harris, T. J. and Peifer, M. (2005). The positioning and segregation of apical

cues during epithelial polarity establishment in Drosophila. *J. Cell Biol.* **170**, 813-823.
Henkemeyer, M. J., Gertler, F. B., Goodman, W. and Hoffmann, F. M. (1987). The Drosophila Abelson proto-oncogene homolog: identification of mutant alleles that have pleiotropic effects late in development. *Cell* **51**, 821-828.
Hernandez, S. E., Settleman, J. and Koleske, A. J. (2004). Adhesion-dependent regulation of p190RhoGAP in the developing brain by the Abl-related gene tyrosine kinase. *Curr. Biol.* **14**, 691-696.
Hoffman, L. M., Jensen, C. C., Kloeker, S., Wang, C. L., Yoshigi, M. and Beckerle, M. C. (2006). Genetic ablation of zyxin causes Mena/VASP mislocalization, increased motility, and deficits in actin remodeling. *J. Cell Biol.* **172**, 771-782.
Irvine, K. D. and Wieschaus, E. (1994). Cell intercalation during Drosophila germband extension and its regulation by pair-rule segmentation genes. *Development* **120**, 827-841.
Koleske, A. J., Gifford, A. M., Scott, M. L., Nee, M., Bronson, R. T., Miczek, K. A. and Baltimore, D. (1998). Essential roles for the Abl and Arg tyrosine kinases in neurulation. *Neuron* **21**, 1259-1272.
Kölsch, V., Seher, T., Fernandez-Ballester, G. J., Serrano, L. and Leptin, M. (2007). Control of Drosophila gastrulation by apical localization of adherens junctions and RhoGEF2. *Science* (in press).
Lanier, L. M. and Gertler, F. B. (2000). From Abl to actin: Abl tyrosine kinase and associated proteins in growth cone motility. *Curr. Opin. Neurobiol.* **10**, 80-87.
Lanier, L. M., Gates, M. A., Witke, W., Menzies, A. S., Wehman, A. M., Macklis, J. D., Kwiatkowski, D., Soriano, P. and Gertler, F. B. (1999). Mena is required for neurulation and commissure formation. *Neuron* **22**, 313-325.
Leptin, M. and Grunewald, B. (1990). Cell shape changes during gastrulation in Drosophila. *Development* **110**, 73-84.
Morize, P., Christiansen, A. E., Costa, M., Parks, S. and Wieschaus, E. (1998). Hyperactivation of the folded gastrulation pathway induces specific cell shape changes. *Development* **125**, 589-597.
Muller, H. A. and Wieschaus, E. (1996). armadillo, bazooka, and stardust are critical for early stages in formation of the zonula adherens and maintenance of the polarized blastoderm epithelium in Drosophila. *J. Cell Biol.* **134**, 149-163.
Nikolaidou, K. K. and Barrett, K. (2004). A Rho GTPase signaling pathway is used reiteratively in epithelial folding and potentially selects the outcome of Rho activation. *Curr. Biol.* **14**, 1822-1826.
Padash Barmchi, M., Rogers, S. and Hacker, U. (2005). DRhoGEF2 regulates actin organization and contractility in the Drosophila blastoderm embryo. *J. Cell Biol.* **168**, 575-585.
Parks, S. and Wieschaus, E. (1991). The Drosophila gastrulation gene concertina encodes a G alpha-like protein. *Cell* **64**, 447-458.
Pilot, F. and Lecuit, T. (2005). Compartmentalized morphogenesis in epithelia: from cell to tissue shape. *Dev. Dyn.* **232**, 685-694.
Rogers, S. L., Rogers, G. C., Sharp, D. J. and Vale, R. D. (2002). Drosophila EB1 is important for proper assembly, dynamics, and positioning of the mitotic spindle. *J. Cell Biol.* **158**, 873-884.
Rogers, S. L., Wiedemann, U., Stuurman, N. and Vale, R. D. (2003). Molecular requirements for actin-based lamella formation in Drosophila S2 cells. *J. Cell Biol.* **15**, 1079-1088.
Rogers, S. L., Wiedemann, U., Hacker, U., Turck, C. and Vale, R. D. (2004). Drosophila RhoGEF2 associates with microtubule plus ends in an EB1-dependent manner. *Curr. Biol.* **14**, 1827-1833.
Sanny, J., Chui, V., Langmann, C., Pereira, C., Zahedi, B. and Harden, N. (2006). *Drosophila* RhoGAP68F is a putative GTPase activating protein for RhoA participating in gastrulation. *Dev. Genes Evol.* **216**, 543-550.
Sweeton, D., Parks, S., Costa, M. and Wieschaus, E. (1991). Gastrulation in Drosophila: the formation of the ventral furrow and posterior midgut invaginations. *Development* **112**, 775-789.
Wang, Y., Miller, A. L., Mooseker, M. S. and Koleske, A. J. (2001). The Abl-related gene (Arg) nonreceptor tyrosine kinase uses two F-actin-binding domains to bundle F-actin. *Proc. Natl. Acad. Sci. USA* **98**, 14865-14870.
Woodring, P. J., Hunter, T. and Wang, J. Y. (2003). Regulation of F-actin-dependent processes by the Abl family of tyrosine kinases. *J. Cell Sci.* **116**, 2613-2626.
Yang, L., Lin, C. and Liu, Z.-R. (2006). P68 RNA helicase mediates PDGF-induced epithelial mesenchymal transition by displacing axin from beta-catenin. *Cell* **127**, 139-155.
Zallen, J. A. and Wieschaus, E. (2004). Patterned gene expression directs bipolar planar polarity in Drosophila. *Dev. Cell* **6**, 343-355.